Large Modulations in the Intensity of Raman-Scattered Light from Pristine Carbon Nanotubes

Adam W. Bushmaker,[1] Vikram V. Deshpande,[2] Scott Hsieh,[2] Marc W. Bockrath,[2] and Stephen B. Cronin[1]
[1]*Department of Electrical Engineering, University of Southern California, Los Angeles, California 90089, USA*
[2]*Department of Applied Physics, California Institute of Technology, Pasadena, California 91125, USA*
(Received 8 January 2009; published 5 August 2009)

Large modulations of up to 2 orders of magnitude are observed in the Raman intensity of pristine, suspended, quasimetallic, single-walled carbon nanotubes in response to applied gate potentials. No change in the resonance condition is observed, and all Raman bands exhibit the same changes in intensity, regardless of phonon energy or laser excitation energy. The effect is not observed in semiconducting nanotubes. The electronic energy gaps correlate with the drop in the Raman intensity, and the recently observed Mott insulating behavior is suggested as a possible explanation for this effect.

DOI: 10.1103/PhysRevLett.103.067401 PACS numbers: 78.67.Ch, 71.30.+h, 73.63.Fg, 78.30.Na

Single-walled carbon nanotubes (SWNTs) provide an excellent system for studying interesting one-dimensional physics, including strong electron-phonon coupling [1,2], ballistic transport [3], and strongly correlated electrons [4–7]. Micro-Raman spectroscopy is a sensitive technique for observing these unique effects [8,9]. Despite the great interest in SWNTs, new phenomena such as those mentioned above are still being discovered with the use of clean, nearly defect-free, suspended SWNTs. Understanding these effects in pristine systems is crucial for the development of SWNT nanodevices.

In this study, the Raman spectra of individual, suspended, pristine quasimetallic (small band gap or ''qm'') SWNTs are found to exhibit changes in intensity by up to 2 orders of magnitude with an applied electrostatic gate voltage (V_g), while for semiconducting nanotubes (sc-SWNTs) the intensity remains constant. The effect is so strong that it renders some qm-SWNTs invisible to Raman spectroscopy and occurs at room temperature over small voltage ranges, suggesting possible device applications in the future. Indeed, there are limited device technologies that have demonstrated the ability to strongly modify a material's optical properties using static electric fields.

It is well known that the Raman intensity of SWNTs is significantly enhanced when one of the photons involved is resonant with an excitonic transition [10–13]. There have been several reports on slight changes in the Raman spectral intensity from SWNTs in response to gate voltages, which were attributed to shifting of the resonance condition [14,15], as well as reports on larger intensity changes in SWNTs under extreme electrolytic doping, due to transition bleaching [16,17] or otherwise anomalous behavior in complex nanotube mats [18]. Raman studies of electrostatically doped graphene have also been undertaken, showing moderate decreases in the 2D band Raman intensity with doping [19].

In contrast to the previous work [14–18], we observe an *increase* in intensity with doping, as opposed to a decrease. Furthermore, this increase occurs with relatively small V_g, in contrast with other studies that used several volts of electrolytic doping or several tens of volts with electrostatic doping. Changes in the resonance condition are ruled out based on the constant Stokes/anti-Stokes intensity ratio and insensitivity to phonon and laser energy. By performing optical and electrical measurements simultaneously, the electrically measured energy gaps (E_{gap}) are compared to the Raman intensity attenuation. Based on these results, the recently observed Mott insulating behavior [20] in qm-SWNTs is suggested as a possible mechanism for the observed behavior.

Recently, there has been a large focus on the Raman G_- band's response to V_g [9,18,21–24]. In these studies, the G_- band frequency and linewidth change drastically due to the influence of the Γ-point Kohn anomaly (KA) in the LO phonon band [25]. These effects were also observed in our devices [24]. The intensity modulation, however, affects all Raman modes universally, not just those associated with the KA. Furthermore, in bands not affected by the KA, no noteworthy shifts or changes in linewidth are observed.

Samples are fabricated using chemical vapor deposition on Pt electrodes with predefined catalyst beds, as reported previously [8,26]. The resulting devices are single-walled nanotubes suspended across trenches 300 nm deep and 2–5 μm wide [see Fig. 1(a)]. The samples in this study were grown using ethanol or methane as the carbon feedstock [27]. No additional processing was performed after the nanotube growth, except for an oxygen bake to rid the devices of amorphous carbon. The devices examined in this study were preselected from many potentially defected or bundled devices by careful examination of the Raman and electrical characteristics, as described below. All nanotubes in this study exhibited a single spatially isolated Raman signal and a high bias saturation current of $\sim 10/L$ (μA), where L is the length in microns [1]. The low temperature transport data from most devices exhibited Coulomb blockade diamonds [4], and all of the devices exhibited little or no D band Raman intensity. These observations indicate that all nanotubes in this study are highly defect-free, individual qm-SWNT devices. Raman spectra were collected from the center of each nanotube in

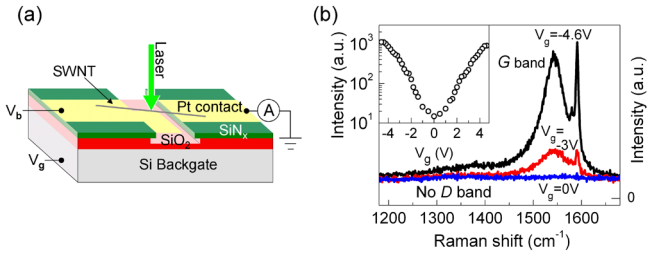

FIG. 1 (color online). (a) Device geometry and (b) G band Raman spectra at various gate voltages, with the inset showing the G_- band intensity as a function of V_g (sample 8B).

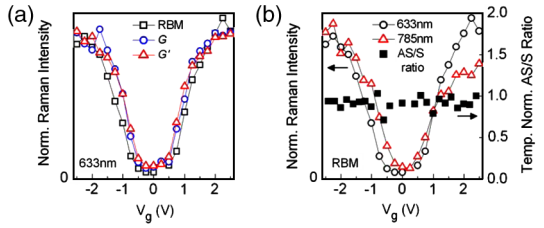

FIG. 2 (color online). (a) Normalized Raman intensities of the RBM, G_+ (TO), and G' bands taken with a 633 nm laser. (b) RBM intensity taken with 633 and 785 nm lasers, together with the RBM AS/S intensity ratio (633 nm, normalized for $T = 300$ K) plotted versus V_g.

the middle of the trench with a Renishaw InVia spectrometer (resolution ~ 1 cm^{-1}) using 532, 633, or 785 nm lasers focused to a diffraction limited spot.

G band Raman spectra taken with a 785 nm laser from an individual, suspended, qm-SWNT are plotted in Fig. 1(b) at several V_g. As with all qm-SWNTs measured in this study, the intensity of the Raman signal increases dramatically with increasing $|V_g|$, varying by up to almost 2 orders of magnitude (>18.8 dB) in this case. Here, the G_+ and G_- bands exhibited an identical intensity change. The G band line shape in Fig. 1(b) is typical of quasimetallic nanotubes, exhibiting a broad, downshifted G_- band, with a sharp G_+ band. Note the near absence of the defect-related D band. A radial breathing mode (RBM) for this nanotube was observed at 173.6 ± 0.5 cm^{-1}, indicating that the diameter of this SWNT is 1.31 nm [28].

Figure 2 shows the Raman data for another nanotube device, including the RBM, G_+ band, and G' band Raman intensities plotted as a function of V_g and the Fermi energy (E_F). The normalized Raman intensity profiles show nearly identical V_g dependences, indicating that this effect affects all of the Raman modes universally, regardless of phonon energy. The G_- band also exhibited the same dependence. The RBM, observed at 153 ± 0.5 cm^{-1} using both 633 and 785 nm lasers, shows similar intensity profiles [Fig. 2(b)], with a Raman signal attenuation of 8.5 dB at $V_g = 0$. Throughout the measurement, the intensity of the background Si 520 cm^{-1} band remained constant. Also shown in the figure is the temperature normalized (300 K) RBM anti-Stokes/Stokes (AS/S) intensity ratio, which is sensitive to changes in the resonance condition [29].

Normally, any changes in the Raman intensity of carbon nanotubes would be due to a change in the resonance condition. However, here we find this is not the case. The resonant Raman intensity of the Stokes process is

$$I^{\mu}(E_L) = C \left| \int \frac{M^{\mathrm{op}} M^{\mathrm{ep}} M^{\mathrm{op}} dk}{[\Delta E][\Delta E - E_{\mathrm{ph}}]} \right|^2, \qquad (1)$$

where C is a constant, $\Delta E = E_L - E_\mu - i\gamma$ is the resonance condition, E_L is the laser energy, E_μ is the excitonic transition energy for the μth subbands, E_{ph} is the phonon energy, γ is the resonance broadening energy, M^{op} is the optical matrix element for the exciton-photon interaction, and M^{ep} is the electron-phonon coupling matrix element [29]. A large change in the Raman intensity can arise from a change in three quantities: (i) the resonance condition ΔE (or $\Delta E - E_{\mathrm{ph}}$), (ii) M^{ep}, or (iii) M^{op}.

We can rule out transition bleaching immediately, as the changes in Fermi energy ($\leq$200 meV) are drastically smaller than the excitonic transition energy (1.5–2.3 eV). It is tempting to attribute the change in Raman intensity to a strain-induced change in resonance [case (i)] caused by the electrostatic gate force [30]. However, this is not the case, since the RBM has a narrow resonance window, and, therefore, small changes in the resonance condition ($E_\mu - E_L$) result in large changes in the RBM AS/S intensity ratio [29], which are not observed [Fig. 2(b)]. Also, the broad G band resonance window would require an unreasonably large change in E_μ to account for such a drastic modulation. Also, we would expect the Raman signal for different phonon modes and laser energies to respond differently to a change in resonance condition, which is not observed [Figs. 2(a) and 2(b)]. Finally, it is statistically unlikely that we would observe a shift *onto* resonance with increasing $|V_g|$ for all 8 nanotubes showing this effect. One would expect some nanotubes to show a shift *off* of resonance with increasing $|V_g|$. We can rule out V_g-induced bending as a cause for the observed intensity modulation, as most suspended nanotubes have slack (and thus bending) as fabricated [31]. Furthermore, the Raman intensity is predicted to decrease with bending [32], opposite the observed behavior. This unanimous evidence suggests that a different mechanism is responsible for the observed behavior.

Ruling out case (i) as a possible explanation, we consider the electron-phonon coupling strength M^{ep} [case (ii)], which is known to be quite different for the various Raman active modes [33]. Therefore, a variation of this quantity is expected to result in different intensity modulation profiles for the RBM, G, and G' bands, which is not observed [Fig. 2(a)]. This is especially true with the G_+ and G_- bands, which have orthogonal TO and LO polarizations in qm-SWNTs, respectively [25]. The electron-phonon coupling of the LO phonon band is influenced by the KA [9,18,21–25] and is drastically different from that of the TO phonon band. Despite this difference, the intensity

behaviors of the TO and LO modes are identical. This leaves a change in the optical matrix element M^{op} [case (iii)] as the only plausible cause of the observed intensity modulation. This intensity modulation appears to be attenuation at small $|V_g|$ rather than enhancement at high $|V_g|$, because the Raman intensity saturates at high $|V_g|$ to a value comparable to that of the sc-SWNTs.

A Raman intensity map of the G band of a third nanotube is plotted in Fig. 3(a), together with the electrically measured conductance. Here the G band peak around 1580 cm^{-1} vanishes near $E_F = 0$. This corresponds to the drop in the conductance observed in the electrical data. The conductance is modeled using the Boltzmann-Landauer (BL) transport equation [24,34], and the Fermi energy is calculated numerically using a geometric gate capacitance C, the Fermi function, and a hyperbolic density of states model [35], according to the equation $E_F + \frac{Q(E_F)}{C} = eV_g$, where Q is the charge induced on the nanotube. This accounts for the quantum capacitance [36] and the band gap, which create a nonlinear $V_g - E_F$ relationship [Fig. 4(b)]. Fitting the data in Fig. 3(a) with this model yielded $C \sim 10$ pF/m and $E_{gap} = 120$ meV. The small offset of the conductance and Raman intensity minima near $V_g = 0$ arises from the gas doping effect [37]. This nanotube exhibits Raman attenuation for $|V_g| < 2$ V and, as with the others, saturation at large V_g. Interestingly, we do not observe this same effect in sc-SWNTs [Fig. 3(b)], which have band gaps on the order of 1 eV. Therefore, the effect is not simply due to a change in the free carrier density.

Out of 9 qm-SWNTs investigated, 8 showed this intensity modulation effect. The Raman intensity of the remaining qm-SWNT was constant. 4 sc-SWNTs were also investigated using this technique, none showing substantial Raman intensity changes with V_g. We, therefore, conclude that the effect is specific to qm-SWNTs. The data for the 8 qm-SWNTs showing this effect are summarized in Table I below. The diameter is given for nanotubes that exhibited a RBM [28]. The G_+/G_- Raman integrated intensity ratios are also listed for each nanotube, giving an indication of the chiral angle ($G_+/G_- = 0 \rightarrow$ zigzag, $G_+/G_- = \infty \rightarrow$ armchair) [22,38]. Also given are the maximum observed Raman attenuation (in dB) and the Fermi energy change corresponding to the FWHM attenuation of the Raman intensity (Δ_{Raman}), found using the $V_g - E_F$ relationship [Fig. 4(b)]. Finally, the energy gaps (E_{gap}) obtained by fitting the BL model to the measured conductance are also given. The correlation between Δ_{Raman} and E_{gap} [Fig. 4(a)] suggests that the observed Raman intensity attenuation is caused by the same effect that causes the electronic energy gaps in qm-SWNTs.

The secondary gap in qm-SWNTs (those with chiral index difference an integer multiple of 3) has long been thought to arise from the curvature of the nanotube, which causes mixing of the π and σ orbitals [38,39]. A Peierls gap transition, one hallmark feature of most one-dimensional metals, was also initially considered. However, density functional theory has found the Peierls gap to be unstable above $T \sim 10^{-8}$ K [25] in all but ultrasmall radius carbon nanotubes [40]. Recently, experimental evidence [20] has confirmed theoretical predictions [41] that, in nearly defect-free qm-SWNTs, a Mott insulator (MI) transition is primarily responsible for creating E_{gap}. In the MI state, strongly correlated electrons localize to their parent atoms, forming gaps of 10–100 meV, even in armchair SWNTs. Raman intensity attenuation has been previously reported for MI transitions in other materials systems [42]. We believe that this same effect is causing the Raman attenuation in these nearly defect-free nanotubes. The fit values for E_{gap} in Table I lie in the range predicted for MI gaps and correlate well with the energy gaps over which the Raman attenuation is observed [Fig. 4(a)], corroborating the MI state.

The Mott insulator transition explains why all of the Raman bands are affected equally under applied gate potentials. In this phase transition, the electrons in the $2p$ orbital of the carbon atom localize to their parent atom through Coulomb repulsion, causing all of the electrons in the π band to be affected, including those involved in excitonic transitions. The details of this interaction are left to future theoretical work. The MI transition also

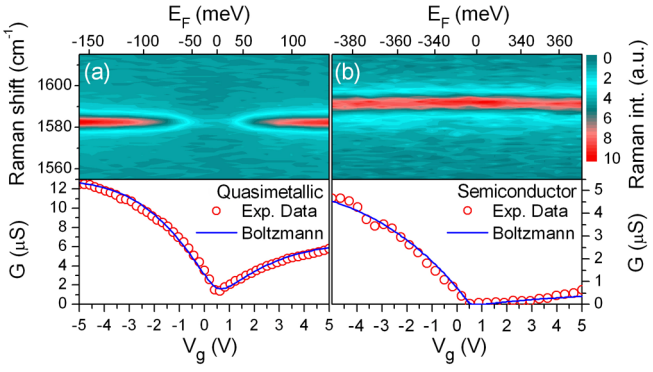

FIG. 3 (color online). The G band spectra and conductance (G) for suspended (a) qm- and (b) sc-SWNTs, plotted versus V_g and E_F. G and E_F are fit using the Boltzmann-Landauer transport model.

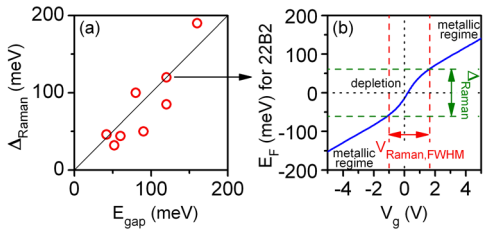

FIG. 4 (color online). (a) Δ_{Raman} plotted versus E_{gap}, determined by fitting the Boltzmann-Landauer transport equation to the experimental data. (b) E_F plotted versus V_g for nanotube 22B2, illustrating the method for determining Δ_{Raman}.

TABLE I. Data summary of qm-SWNTs showing intensity modulation. Listed values include nanotube diameter, G_+/G_- integrated Raman intensity ratio, maximum Raman attenuation, attenuation energy gap (Δ_{Raman}), and electronic gap (E_{gap}).

Sample	Diameter (nm)	G_+/G_- int. rat.	Att. (dB)	Δ_{Raman} (meV)	E_{gap} (meV)
22B1	···	0.04	12.8	50	90
13B	···	0.12	0.8	85	120
8B	1.31	0.08	>18.8	190	160
18B	1.48	0.40	8.5	44	60
22B2	···	$\rightarrow \infty$	11.8	120	120
19B	···	$\rightarrow \infty$	11.5	32	52
5A	1.97	$\rightarrow 0$	13.8	46	42
5B	···	$\rightarrow 0$	7.3	100	80

accounts for the qm/sc difference, because in sc-SWNTs, the electronic gap originates from confinement effects. Absorption studies (optical [43] and x-ray [44]) in other materials systems have also shown dramatic changes as a result of the MI transition. Finally, the gate voltage-induced MI transition has already been exploited in cuprate MI field effect transistors [45]. It is likely that this modulation has not been observed until now because most gate voltage experiments with qm-SWNTs are performed on nanotube-on-substrate devices rather than pristine, suspended devices. The MI state requires the presence of a well-defined charge neutrality point [20], which may not occur in samples with defects, substrate contact, or post-processing residue. This may be the case where, as mentioned above, one nanotube out of a total of nine that were measured failed to show this effect. It is possible that this one metallic nanotube had a finite defect density or was in a bundle and slipped by the prescreening process, indicating that this effect may be used to characterize qm-SWNTs.

In conclusion, we observe a large attenuation of the Raman signal from individual pristine, suspended quasimetallic SWNTs by up to 2 orders of magnitude near zero electrostatic gating, while semiconducting SWNTs do not exhibit the effect. The attenuation is so strong as to render some qm-SWNTs undetectable by Raman spectroscopy without a gate voltage. Changes in the resonance condition and transition bleaching are ruled out on the basis of the constant anti-Stokes/Stokes intensity ratio and behavior with respect to different phonon modes and laser energies. The recently observed Mott insulator transition in qm-SWNTs is suggested as a possible mechanism for the changes in the Raman intensity. The Raman attenuation energy gaps for 8 nanotubes are compared to the electronic energy gaps, estimated from fits to the Boltzmann-Landauer transport model, and show correlation consistent with the Mott insulator picture.

This research was supported in part by DOE Grant No. DE-FG02-07ER46376 and the National Science Foundation Graduate Research Program.

[1] E. Pop *et al.*, Phys. Rev. Lett. **95**, 155505 (2005).
[2] M. Lazzeri *et al.*, Phys. Rev. Lett. **95**, 236802 (2005).
[3] J. Kong *et al.*, Phys. Rev. Lett. **87**, 106801 (2001).
[4] V. V. Deshpande and M. Bockrath, Nature Phys. **4**, 314 (2008).
[5] M. Bockrath *et al.*, Nature (London) **397**, 598 (1999).
[6] B. Dora *et al.*, Phys. Rev. Lett. **99**, 166402 (2007).
[7] H. Ishii *et al.*, Nature (London) **426**, 540 (2003).
[8] A. W. Bushmaker *et al.*, Nano Lett. **7**, 3618 (2007).
[9] J. C. Tsang *et al.*, Nature Nanotech. **2**, 725 (2007).
[10] M. S. Dresselhaus *et al.*, Carbon **40**, 2043 (2002).
[11] F. Wang *et al.*, Science **308**, 838 (2005).
[12] A. Jorio, M. S. Dresselhaus, and G. Dresselhaus, *Carbon Nanotubes: Advanced Topics in the Synthesis, Structure, Properties and Applications* (Springer, New York, 2008).
[13] V. Perebeinos, J. Tersoff, and P. Avouris, Phys. Rev. Lett. **92**, 257402 (2004).
[14] P. M. Rafailov *et al.*, Phys. Rev. B **72**, 045411 (2005).
[15] S. B. Cronin *et al.*, Appl. Phys. Lett. **84**, 2052 (2004).
[16] L. Kavan *et al.*, J. Phys. Chem. B **105**, 10 764 (2001).
[17] P. Corio *et al.*, Chem. Phys. Lett. **370**, 675 (2003).
[18] A. Das *et al.*, Phys. Rev. Lett. **99**, 136803 (2007).
[19] A. Das *et al.*, Nature Nanotech. **3**, 210 (2008).
[20] V. V. Deshpande *et al.*, Science **323**, 106 (2009).
[21] N. Caudal *et al.*, Phys. Rev. B **75**, 115423 (2007).
[22] Y. Wu *et al.*, Phys. Rev. Lett. **99**, 027402 (2007).
[23] H. Farhat *et al.*, Phys. Rev. Lett. **99**, 145506 (2007).
[24] A. W. Bushmaker *et al.*, Nano Lett. **9**, 607 (2009).
[25] S. Piscanec *et al.*, Phys. Rev. B **75**, 035427 (2007).
[26] J. Cao *et al.*, Small **1**, 138 (2005).
[27] L. M. Huang *et al.*, J. Phys. Chem. B **110**, 11 103 (2006).
[28] P. T. Araujo *et al.*, Phys. Rev. B **77**, 241403(R) (2008).
[29] C. Fantini *et al.*, Phys. Rev. Lett. **93**, 147406 (2004).
[30] E. D. Minot *et al.*, Phys. Rev. Lett. **90**, 156401 (2003).
[31] V. Sazonova *et al.*, Nature (London) **431**, 284 (2004).
[32] S. Malola, H. Hakkinen, and P. Koskinen, Phys. Rev. B **78**, 153409 (2008).
[33] J. Jiang *et al.*, Phys. Rev. B **72**, 235408 (2005).
[34] M. J. Biercuk *et al.*, Top. Appl. Phys. **111**, 455 (2008).
[35] M. Bockrath *et al.*, Science **275**, 1922 (1997).
[36] P. J. Burke, IEEE Trans. Nanotechnol. **1**, 129 (2002).
[37] V. Derycke *et al.*, Appl. Phys. Lett. **80**, 2773 (2002).
[38] X. Blase *et al.*, Phys. Rev. Lett. **72**, 1878 (1994).
[39] C. Zhou, J. Kong, and H. Dai, Phys. Rev. Lett. **84**, 5604 (2000).
[40] D. Connetable *et al.*, Phys. Rev. Lett. **94**, 015503 (2005).
[41] L. Balents and M. P. A. Fisher, Phys. Rev. B **55**, R11 973 (1997).
[42] T. Katsufuji and Y. Tokura, Phys. Rev. B **50**, 2704 (1994).
[43] M. Nakamura *et al.*, Phys. Rev. B **75**, 155103 (2007).
[44] C. T. Chen *et al.*, Phys. Rev. Lett. **66**, 104 (1991).
[45] D. M. Newns *et al.*, J. Electroceram. **4**, 339 (2000).